Similarity Analysis of Thermal Flow between Prototype and Scale Model for Ventilated Storage Cask

Ju-Chan Lee, Kyung-Sik Bang, Seung-Hwan Yu and Woo-Seok Choi
Korea Atomic Energy Research Institute (KAERI)
989-111 Daedeok-daero, Yuseong-Gu, Daejeon, 34057, Republic of Korea
sjclee@kaeri.re.kr

Abstract
The weight of a spent nuclear fuel concrete storage cask is usually over 100 tons, and thermal testing using a prototype cask is expensive and time consuming. In this study, thermal testing using a scaled-down model is proposed to efficiently perform the thermal testing of the storage casks. Scaling analyses were performed to derive the scale ratios between the prototype and the half-scale model. Thermal analysis and testing were carried out to verify the reliability of the scale ratios and the similarity of the scaled-down model. The analysis results showed that the scale ratios were conserved well between the prototype and the half-scale model. The analysis results agreed well with the test results. From the results of thermal tests, thermal flow similarity has been demonstrated between the prototype cask and the half-scale model.

1. Introduction

Spent nuclear fuel emits strong radiation and decay heat for a long period of time. Therefore, in a spent fuel storage system, the shielding, criticality, thermal, structural, and containment integrity must be maintained throughout the design life. In particular, the thermal integrity of the spent fuel, shielding, and sealing materials should be maintained by minimizing the temperature inside the storage system considering the natural cooling system.

Concrete casks are widely used worldwide for the storage of spent nuclear fuel. These concrete casks are typically about 6 meters in height and 3 meters in diameter, and they weigh 140 tons or more when loaded. A full scale model is required to accurately simulate the heat transfer and flow phenomenon of the cask. However, full-scale testing of large-scale casks is time consuming and very expensive. A scaled-down model facilitates time and cost effective test evaluation of large casks. In this study, a thermal test method using a scaled-down model was investigated for the efficient thermal testing of storage casks.

Concrete cask has been developed for the storage of 21 PWR spent nuclear fuel assemblies. The cask consists of a canister for loading the spent fuel and a concrete over-pack for radiation shielding. Removal of decay heat from the spent fuel is a key parameter for the design and operation of a cask. In general, dry storage casks rely on heat conduction and natural convection for the removal of decay heat. Concrete has lower thermal conductivity than metal. Therefore, a passive cooling system is introduced in the cask to properly remove the decay heat from the spent fuel. Four air inlet and outlet ducts are installed at the bottom and top of the concrete over-pack, and an air flow path is formed between the canister and the concrete over-pack so that external air circulates inside the cask. The purpose of this study is to derive the scale ratios and to verify the thermal flow similarity between the prototype and the scaled-down model.

2. Scaling analysis of storage cask

The decay heat generated from the spent fuel is transferred to the outside by natural convection through the air flow path, conduction through the cask body, and convection & radiation at the cask surface. Scaling analyses were performed to derive the scale ratios for three heat transfer modes, namely, convection through the air flow path, conduction through the cask body, and a combination of convection and conduction through the air path and the cask body.

2.1 Convective heat transfer mode

Scale ratios for convective heat transfer mode in which all decay heat is removed through the air flow path are derived as follows [1]. In this condition, the temperature of air outlet is conserved between the full-scale and scaled-down model.

- Heat flux and volumetric heat source:

$$q'' = \frac{q}{\pi DH},\ \dot{q} = \frac{q}{A_c H},\ [q'']_R = [\dot{q} \times L_c]_R,\ [\dot{q}]_R = \left[\frac{q''}{L_c}\right]_R \quad (1)$$

- Heat transfer rate through the air outlet:

$$q = \dot{m}\, C_p(\Delta T) = \rho\, u\, A_f \times C_p\, (\Delta T),\ [q]_R = [\dot{m}]_R\ ([\Delta T]_R = 1) \quad (2)$$

- Temperature deference between the air inlet and outlet:

$$\Delta T = \frac{q}{\dot{m}\, C_p} = \frac{\dot{q} \times A_c H}{\rho\, u\, A_f \times C_p},\ [\Delta T]_R = \left[\frac{\dot{q} \times A_c H}{\rho\, u\, A_f \times C_p}\right]_R = \left[\frac{\dot{q} H}{u}\right]_R = 1.0 \quad (3)$$

- Scale ratio for volumetric heat source:

$$[\dot{q}]_R = \left[\frac{u}{H}\right]_R = \left[\frac{u}{L_c}\right]_R \quad (4)$$

- Buoyancy and pressure drop due to friction along the air path:

$$-\Delta p = \rho\beta(\Delta T) g H_p = \frac{1}{2}\rho u^2 f \frac{H}{D_h}\left(\Delta T = \frac{\dot{q} \times A_c H}{\rho\, u\, A_f \times C_p}\right) \quad (5)$$

$$u^3 = 2g\beta \frac{\dot{q}}{\rho\, C_p} \frac{A_c}{A_f} H_p \times \frac{D_h}{f} \quad (6)$$

- Scale ratio for the velocity of air:

$$[u]_{ratio} = \left[\left(2g\beta \frac{\dot{q}}{\rho\, C_p} \frac{A_c}{A_f} H_p \times \frac{D_h}{f}\right)^{1/3}\right]_R = \left[\left(\dot{q} H_p D_h\right)^{1/3}\right]_R = \left[\left(\dot{q} {L_c}^2\right)^{1/3}\right]_R$$
$$= \left[(u\, L_c)^{1/3}\right]_R = \left[{L_c}^{1/2}\right]_R = 0.707 \quad (7)$$

- Scale ratios for the heat source mass flow rate:

$$[\dot{q}]_R = \left[\frac{u}{L_c}\right]_R = \left[\frac{{L_c}^{1/2}}{L_c}\right]_R = \left[\frac{1}{{L_c}^{1/2}}\right]_r = 1.414 \quad (8)$$

$$[q'']_R = [\dot{q}\, L_c]_R = \left[{L_c}^{1/2}\right]_R = 0.707 \quad (9)$$

$$[q]_R = \left[\dot{q}\, {L_c}^3 H\right]_R = \left[{L_c}^{5/2}\right]_R = 0.177 \quad (10)$$

$$[\dot{m}]_R = [q]_R = \left[{L_c}^{5/2}\right]_R = 0.177 \quad (11)$$

2.2 Conduction transfer mode

Scale ratios are derived for conduction heat transfer mode in which the decay heat is removed to the outside by thermal conduction through the cask body, and convection and radiation at the cask surface. In this condition, the cask surface temperature is conserved between the full-scale and scaled-down model.

- Governing equation of heat transfer at cask surface:

$$q" = h(T_s - T_a) + \sigma\varepsilon(T_s^4 - T_a^4),\ [q'']_R = [T_s - T_a]_R = 1.0 \quad (12)$$

- Equation of thermal conduction:

$$q" = k\frac{(T_i - T_o)}{L_c},\ [q'']_R = \left[\frac{T_i - T_o}{L_c}\right]_R = 1.0 \quad (13)$$

- Scale ratio for temperature difference of inner and outer walls:

$$[T_i - T_o]_R = [L_c]_R = 0.5 \quad (14)$$

2.3 Combined heat transfer mode

Scale ratios are derived for combined heat transfer mode in which all decay heat is removed by convection through the air path and conduction of the cask body. In a real cask, decay heat from spent fuel is removed through the air flow path and the cask body. In the full-scale and half-scale model, 76.7 % and 63.6 % of the heat is removed by convection through the air path. A correction factor is introduced to compensate for heat loss through the cask body.

- Heat transfer rates through air flow path for prototype and half-scale model:

$$q_p = (0.767q_p + 0.233q_p),\ q_h = (0.636q_h + 0.364q_h) \quad (15)$$

- Heat source correction factor (α)

$$\alpha q_h = \alpha(0.636q_h + 0.364q_h),\ \alpha = \frac{q_{p(f)}}{q_{h(f)}} = \frac{0.767}{0.636} = 1.206 \quad (16)$$

The scale ratios of heat sources for the combined heat transfer mode are calculated by multiplying the scale ratios from the convective heat transfer mode by the heat source correction factor:

$$[\dot{q}]_R = \left[\frac{1}{L_c{}^{1/2}}\right]_R \alpha = \sqrt{2} \times 1.206 = 1.705 \quad (17)$$

$$[q'']_R = \left[L_c{}^{1/2}\right]_R \alpha = \frac{1}{\sqrt{2}} \times 1.206 = 0.853 \quad (18)$$

$$[q]_R = \left[L_c{}^{5/2}\right]_R \alpha = \frac{1}{\sqrt{2^5}} \times 1.206 = 0.213 \quad (19)$$

The scale ratios for the velocity and mass flow rate at the air inlet and outlet are the same as the scale ratios from the convective heat transfer mode. Table 1 summarizes the scale ratios of the half-scale model for the three heat transfer modes. In the convective heat transfer mode, the scale ratio of the heat flux to preserve the air outlet temperature is derived as 0.707. The scale ratios for the velocity and the mass flow rate of the air outlet are derived as 0.707 and 0.177, respectively. In the conduction heat transfer mode, the scale ratio of the heat flux to preserve the temperature of the cask surface is derived as 1.0. At this time, the scale ratio of the temperature difference between the inner and outer walls of the cask is 0.5. In the combined heat transfer mode, the scale ratio of the heat flux is calculated as 0.853 by multiplying the correction factor in the scale ratio obtained from the convective heat transfer mode.

3. Similarity analysis of storage cask

3.1 Analysis model

ANSYS FLUENT Ver.19 [2] is used for the thermal analysis of the cask. Fig. 1 shows the heat transfer mechanism and thermal analysis model for the concrete cask. In the analysis model, the fuel basket inside the canister is excluded. The heat source from the spent fuel is considered as the heat flux on the surface of canister. Heat from the canister surface is primarily removed by natural convection due to the buoyancy-driven air flow between the canister and the concrete over-pack. The air inlet and outlet ducts allow air circulation through the air flow path. Heat transfer through the cask body is done by heat conduction. Heat is dissipated from the outer surface of the cask to the environment by convection and radiation.

The area surrounding a storage cask is classified as a turbulent region under normal operating condition. The convective heat transfer coefficients by the atmosphere in the vertical cylinder and horizontal surface are defined by the following equations [3]:

- Side of the cask (vertical cylinder)

$$h_{nc} = 1.31(\Delta T)^{1/3} \quad (20)$$

- Upper surface of the cask (horizontal plate)

$$h_{nc} = 1.52(\Delta T)^{1/3} \quad (21)$$

Radiation heat transfer at the cask surface is affected by the emissivity of the material. The outer surface of the concrete over-pack is lined with carbon steel, and the lining surface is coated by splaying with aluminum. When aluminum is in contact with air, an oxide film is formed to prevent corrosion. The emissivity range of aluminum oxide is from 0.26 to 0.42 [4]. The surface emissivity was applied as 0.4.

The half-scale model has the same shape as the prototype cask, reducing the dimension to 1/2. Table 2 shows the analysis conditions for the three heat transfer modes of the prototype and the half-scale model. The ambient temperature was considered as 20 ℃ for all analysis conditions.

3.2 Similarity analysis

Thermal analyses were carried out for the prototype cask and the half-scale model to verify the reliability of the scale ratios obtained from the scaling analysis. Fig. 2 shows the temperature contours of the prototype cask for the three heat transfer modes. Fig. 3 shows the radial

temperature distributions of the prototype cask for the three heat transfer modes. In the convective heat transfer mode, the temperature of the upper part is higher than that of the lower part due to the effect of natural convection. In the conduction heat transfer mode, the temperature of the middle part of the cask is higher than those of the upper and lower parts. Considering only the conduction through the cask body, a sudden temperature variation in the radial direction is observed.

Tables 3 to 5 show the similarity analysis results for the prototype and the half-scale model for the three heat transfer modes. The scale ratios of the main parameters (temperature, velocity, and mass flow rate) correspond with the scaling analysis results in the range of 3 % between the prototype and the half-scale model. Therefore, the reliabilities of the scale ratios have been proved for the three heat transfer modes. In the convection and conduction heat transfer modes, relatively large temperature differences are observed between the prototype and the half-scale model. However, a similar temperature distribution is observed in the combined heat transfer mode with the heat source correction factor.

Thermal analyses were performed under the conditions that the heat sources of the three heat transfer modes were applied to the real cask considering convection through the air flow path and conduction through the cask body. Table 6 shows the CFD analysis results obtained for the prototype and half-scale model with three heat sources. When the heat source of 2.969 kW obtained from the convection mode is applied, the temperature of scale-down model is lower than that of the prototype. On the other hand, when the heat source of 4.200 kW obtained from the conduction mode is applied, the temperature of scaled-down model is higher than that of the prototype. When the heat source of 3.583 kW obtained from the scaling analysis of the combined mode is applied, the temperature of the scaled-down model is similar to that of the prototype. Therefore, thermal flow similarity was maintained only in the combined mode.

4. Thermal test and verification of similarity

4.1. Thermal test equipment

A full-scale prototype cask and a half-scale model were fabricated for the thermal tests. The half-scale model has the same shape as the prototype cask, and the dimensions are reduced by 1/2. One electric heater rod was installed in the canister to simulate the decay heat from spent fuel. The total thermal power was considered to be 16.8 kW for the prototype cask. In the half-scale model, the total heat sources were considered to be 2.969 kW and 3.583 kW, which were derived from the scaling analysis. Fig. 4 shows the thermal test model and facility for the prototype cask. A total of 80 thermocouples were installed in the test model, and 16 thermocouples were installed to measure the ambient temperatures. Hot wire and vane-type anemometers were installed at the air inlet and outlet ducts to measure the velocities.

4.2 Comparison of thermal test and analysis results

Thermal tests were performed for the prototype and the half-scale model to verify the reliability of the thermal analysis results. Table 7 shows a comparison of the thermal test and analysis results for the prototype cask under an ambient temperature of 16 ℃. The thermal test results showed similar temperature profiles to that of the analysis results. The analysis results were slightly higher than the test results. The calculated temperatures were within 7.8 % in the canister, 2.7 % in the inner surface of the over-pack, and 8.6 % in the outer surface of the over-pack, compared to the measured temperature. The temperatures and velocities at the air inlet and outlet ducts were similar to each other except the velocity at the air inlet. The measurement range of the hot wire anemometer is 0 to 20 m/s. The velocity of the air inlet was analyzed to be out of the measurement range of the anemometer. The heat removal rates by convection through the air flow path were calculated as 74.3% and 77.3% in the thermal test and analysis, respectively. The test results are in good agreement with the analysis results. Thus, it was confirmed that the thermal analyses successfully estimated the temperatures of the cask.

4.3 Verification of thermal flow similarity

The thermal test results of the prototype and the half-scale were compared to verify the thermal flow similarity of the scaled-down model. Table 8 shows a comparison of the test results between the prototype and the half-scale model. The temperatures of the half-scale model with the heat source of 3.583 kW are similar to those of the prototype cask. The air outlet temperature of the scaled-down model shows 3 % difference with that of the prototype cask. The velocity ratios of the air inlet and outlet ducts are 0.714 and 0.692, which are within the difference of 3 % with the velocity scale ratio of 0.707 obtained from the scaling analysis. The mass flow rate ratio through the air outlet of the half-scale model consistent with the scale ratio of 0.177 obtained from the scaling analysis. Therefore, thermal flow similarity was demonstrated between the prototype and the half-scale model with a heat source correction factor. In particular, it is possible to predict the overall temperature distributions of the prototype cask by using the half-scale model. Therefore, the validity of thermal testing using the scaled-down model has been proved. In the half-scale model, the heat transfer rate through the air flow path is reduced by more than 10 % compared to the prototype cask because convection heat transfer efficiency is reduced in the scaled-down model.

5. Conclusion

Scaling analyses were performed to estimate the heat source for thermal testing using a scaled-down model. Scaling ratios were derived for the three heat transfer modes of convection, conduction, and a combination of convection and conduction. Thermal analyses were performed for the prototype cask and the half-scale model for the three heat transfer modes. The scale ratios of the main parameters corresponded with the scaling analysis results. Therefore, the reliability of the scale ratios has been proved. In the combined heat transfer mode, the temperatures of the half-scale model were similar to those of the prototype cask. Therefore, the thermal flow similarity was proved only in the combined heat transfer mode. Thermal tests were performed for the prototype and the half-scale model to verify the reliability of the thermal analysis results and the thermal flow similarity of the scaled-down model. There was good agreement between the thermal test and analysis results. In the thermal test results, the scale ratios of the temperature and velocity at the air outlet were consistent with the scaling analysis results. Therefore, the validity of thermal testing using the scaled-down model has been proved. The results of this study can be used as basic data for the thermal testing of storage casks using a scaled-down model.

References

[1] H.M. Kim et al., “Development of scaling laws of heat removal and CFD assessment in concrete cask air path”, Nuclear Engineering and Design, 278 (2014).

[2] ANSYS Inc., “ANSYS FLUENT User's Guide”, ANSYS Fluent, Ver.19, 2018.

[3] J.P. Holman, “Heat Transfer”, International Student Edition 8th Ed., 533, 2000.

[4] MIKRON, “Table of Emissivity of Various Surfaces”, MIKRON Instruments Company, Inc.

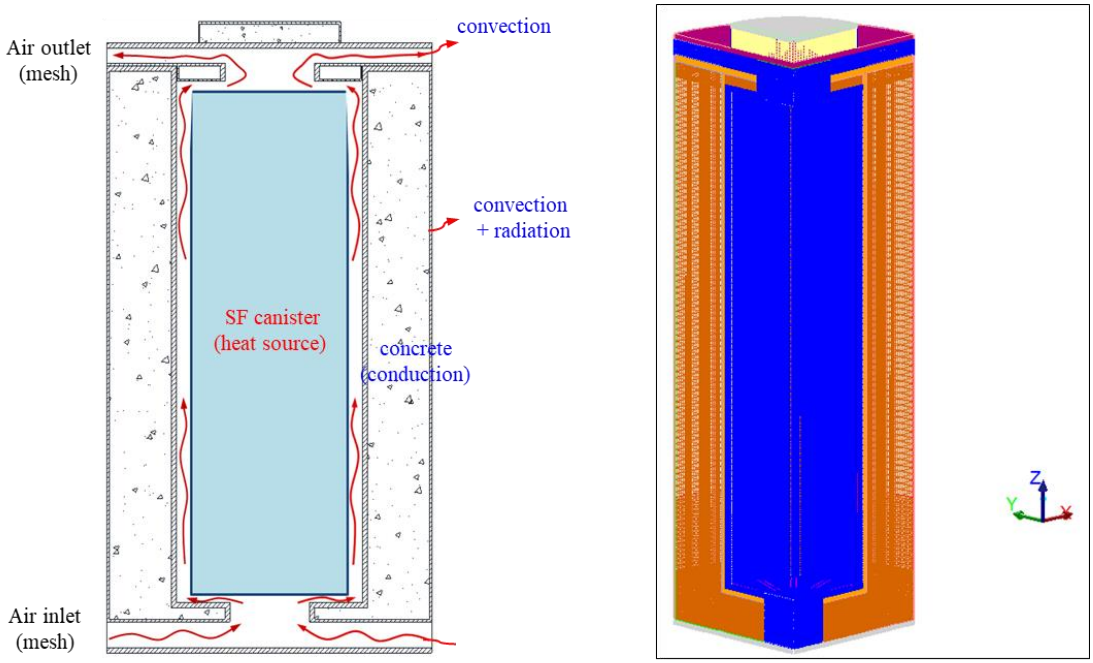

(a) Heat transfer mechanism (b) Thermal analysis model

Fig. 1. Heat transfer mechanism and thermal analysis model of concrete cask

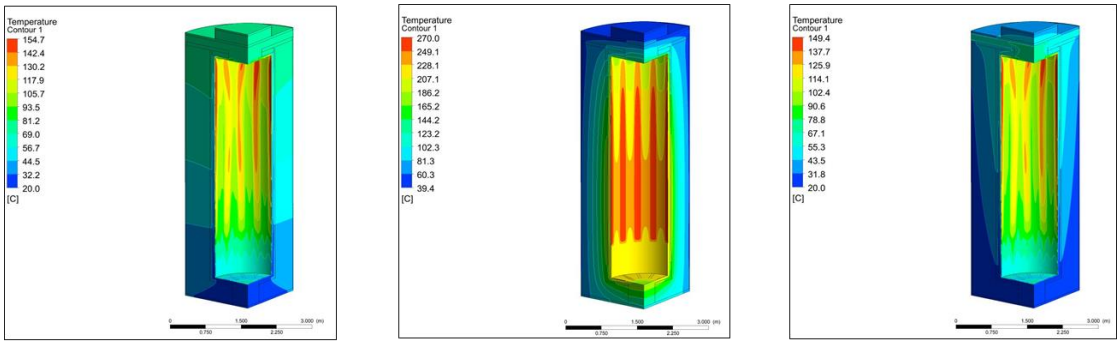

(a) Convection mode **(b) Conduction mode** **(c) Combined mode**

Fig. 2. Temperature contours of prototype cask for three heat transfer modes

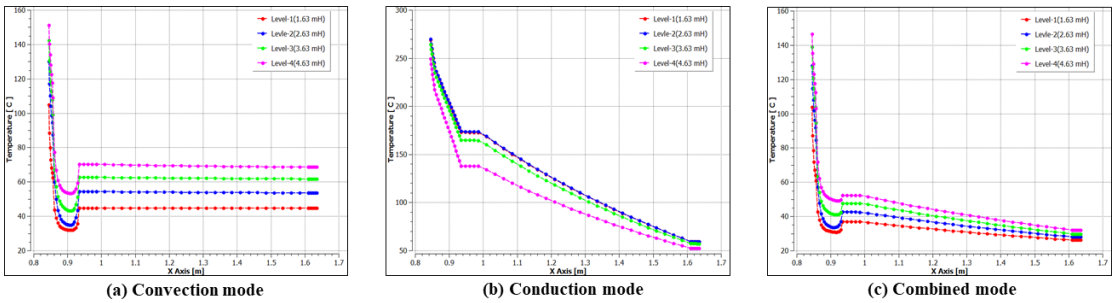

(a) Convection mode **(b) Conduction mode** **(c) Combined mode**

Fig. 3. Temperature profiles of prototype cask for three heat transfer modes

(a) Thermal test model (b) Thermal test facility

Fig. 4. Thermal test model and facility for prototype cask

Table 1. Scale ratios of half-scale model for three heat transfer modes

Scaling parameters	Heat transfer modes		
	Convection	Conduction	Combined
Length scale, $[L]_R$	0.5	0.5	0.5
Temp. difference between air inlet and outlet $[\Delta T]_R$	1.0	-	1.0
Temp. difference of cask inner and outer walls, $[\Delta T]_R$	-	0.5	-
Volumetric heat generation rate, $[\dot{q}]_R$	$\sqrt{2} = 1.414$	2.0	$\sqrt{2}\alpha = 1.705$
Heat flux, $[q'']_R$	$\frac{1}{\sqrt{2}} = 0.707$	1.0	$\frac{1}{\sqrt{2}}\alpha = 0.853$
Heat source, $[q]_R$	$\frac{1}{\sqrt{2^5}} = 0.177$	0.25	$\frac{1}{\sqrt{2^5}}\alpha = 0.213$
Velocity, $[u]_R$	$\frac{1}{\sqrt{2}} = 0.707$	-	$\frac{1}{\sqrt{2}} = 0.707$
Mass flow rate, $[\dot{m}]_R$	$\frac{1}{\sqrt{2^5}} = 0.177$	-	$\frac{1}{\sqrt{2^5}} = 0.177$

Table 2. CFD analysis conditions for three heat transfer modes

Heat transfer modes	Heat source (kW)			Heat flux (W/㎡)		
	Prototype	Model	Ratio	Prototype	Model	Ratio
Convection	16.8	2.969	0.177	553	391	0.707
Conduction	16.8	4.200	0.250	553	553	1.000
Combined	16.8	3.583	0.213	553	472	0.853

Table 3. CFD analysis results of prototype and half-scale model for convection mode

	Prototype	Half-scale	Ratio
Total heat source (kW)	16.8	2.97	0.177
Heat flux from canister (W/㎡)	553	391	0.707
Temp. of air inlet (℃)	20.0	20.0	1.000
Temp. of air outlet (℃)	74.6	74.2	0.995 (~1.0)
Velocity of air inlet (m/s)	0.66	0.45	0.682 (~0.707)
Velocity of air outlet (m/s)	0.80	0.56	0.700 (~0.707)
Mass flow rate (kg/s)	0.3051	0.0525	0.172 (~0.177)
Temp. of canister surface (℃)	101.1	90.0	0.890
Temp. of cask inner wall (℃)	56.1	53.8	0.959
Temp. of cask surface (℃)	55.2	53.6	0.971
Average cask temp. (℃)	54.3	53.1	0.978

Table 4. CFD analysis results of prototype and half-scale model for conduction mode

	Prototype	Half scale	Ratio
Total heat source (kW)	16.8	4.2	0.25
Heat flux from canister (W/㎡)	553	553	1.0
Temp. of cask inner wall (℃)	158.7	107.2	0.675
Temp. of cask outer surface (℃)	57.2	57.0	0.997 (~1.0)
Temp. difference between cask inner and outer walls (℃)	101.5	50.2	0.495 (~0.5)
Temp. of canister surface (℃)	226.3	190.5	0.842
Average cask temp. (℃)	103.5	81.9	0.791

Table 5. CFD analysis results of prototype and half scale for combined mode

	Prototype	Half scale	Ratio
Total heat source (kW)	16.8	3.583	0.213
Heat flux from canister (W/㎡)	553	472	0.853
Temp. of air inlet (℃)	20.0	20.0	1.000
Temp. of air outlet (℃)	63.9	62.8	0.983 (~1.0)
Velocity of air inlet (m/s)	0.63	0.44	0.698 (0.707)
Velocity of air outlet (m/s)	0.74	0.52	0.703 (0.707)
Mass flow rate (kg/s)	0.2920	0.0509	0.174 (0.177)
Average temp. of cask (℃)	36.0	37.6	1.044
Temp. of canister surface (℃)	97.0	94.4	0.973
Temp. of cask inner wall (℃)	43.6	42.5	0.975
Temp. of cask surface (℃)	29.2	32.2	1.102
Heat transfer rate through air path (kW)	12.890 (76.7 %)	2.278 (63.6 %)	

Table 6. CFD analysis results of prototype and half-scale model with three heat sources

Item	Prototype (16.8 kW)	Half-scale model		
		2.969 kW	3.583 kW	4.200 kW
Heat flux from canister (W/㎡)	553	391	472	553
Temp. of air inlet (℃)	20.0	20.0	20.0	20.0
Temp. of air outlet (℃)	63.9	57.0	62.8	68.5
Velocity of air inlet (m/s)	0.63 s	0.42	0.44	0.46
Velocity of air outlet (m/s)	0.74	0.49	0.52	0.55
Mass flow rate (kg/s)	0.2920	0.0483	0.0508	0.0531
Temp. of canister surface (℃)	97.0	84.4	94.4	103.9
Temp. of cask inner wall (℃)	43.6	39.3	42.5	45.7
Temp. of cask surface (℃)	29.2	30.6	32.2	33.7
Average temp. of cask (℃)	36.0	35.2	37.6	40.0
Heat transfer rate through air path (kW)	12.890 (76.7 %)	1.870 (63.0 %)	2.278 (63.6 %)	2.689 (64.0 %)

Table 7. Comparison of thermal test and analysis results for prototype cask

Item		Test	Analysis	Difference (%)
Canister (℃)		112.0	120.8	7.8
Over-pack inside (℃)		41.5	42.6	2.7
Concrete (℃)		31.7	33.3	5.0
Over-pack outside (℃)		23.9	26.0	8.6
Air inlet	Temperature (℃)	12.6	12.6	0.0
	Velocity (m/s)	0.42	0.56	33.3
Air outlet	Temperature (℃)	59.4	61.1	2.8
	Velocity (m/s)	0.65	0.67	3.0
	Mass flow rate (kg/s)	0.2650	0.2654	1.5
Heat transfer rate by convection through duct (kW)		12.488	12.989	4.0

Table 8. Comparison of thermal test results between prototype and half-scale model

Item		Prototype	Half-scale model	
			q = 2.969 kW	q = 3.583 kW
Canister (℃)		112.0	94.3	105.3
Over-pack inside (℃)		41.5	38.2	42.2
Concrete (℃)		31.7	28.8	32.3
Over-pack outside		23.1	24.8	26.6
Air inlet	Temperature (℃)	12.6	12.6	12.6
	Velocity (m/s)	0.42	0.26 (0.619)	0.30 (0.714)
Air outlet	Temperature (℃)	59.4	54.2 (0.912)	61.3 (1.032)
	Velocity (m/s)	0.65	0.41 (0.631)	0.45 (0.692)
	Mass flow rate (kg/s)	0.2650	0.0420 (0.158)	0.0456 (0.172)

Heat transfer rate by convection through duct (kW)	12.488 (74.3 %)	1.761 (59.3 %)	2.236 (62.5 %)